Identification of distinct functional microstructural domains controlling C storage in soil

Markus Steffens[1,2]*, Derek Rogge[3], Carsten W. Mueller[1], Carmen Höschen[1], Johann Lugmeier[1], Angelika Kölbl[1], Ingrid Kögel-Knabner[1,4]

[1]*Lehrstuhl für Bodenkunde, Wissenschaftszentrum Weihenstephan, Technische Universität München, Emil-Ramann-Str. 2, D-85354 Freising, Germany*

[2]*Department of Soil Sciences, Research Institute of Organic Agriculture (FiBL), Ackerstrasse 113, CH-5070 Frick, Switzerland*

[3]*Applied spectroscopy group, Deutsche Forschungsanstalt für Luft- und Raumfahrt Oberpfaffenhofen, D-82234 Wessling, Germany*

[4]*Institute of Advanced Study, Technische Universität München, Lichtenbergstraße 2a, D-85748 Garching, Germany*

*markus.steffens@fibl.org

Table S1: Characteristics of the 18 mass signature classes identified in seven images of the pure standard materials iron oxide (Goethite with different degrees of Al-substitution), aluminum oxide (Boehmite), and phyllosilicates (Illite and Montmorillonite; Figure S1). All standard materials were attached on adhesive carbon film. Mean normalized counts (MNC) give the average MNC values of all pixels that were assigned to a given mass signature class (compare figure S2). Ratios were calculated with the average MNC values.

Mass signature class	Mean normalized counts [MNC]						Ratios						Compound groups	Colour
	^{12}C	^{16}O	^{28}Si	$^{27}Al^{16}O$	$^{56}Fe^{16}O$	$^{56}Fe^{16}O_2$	C/O	Si/Al	Fe/Al	Si/O	Al/O	Fe/O		
1	5.4477	0.5210	0.0048	0.0112	0.0105	0.0048	10.46	0.42	1.37	0.01	0.02	0.03	Carbon film	
2	3.8785	1.9885	0.0077	0.0472	0.0492	0.0289	1.95	0.16	1.65	0.00	0.02	0.04		
3	2.0208	3.6100	0.0099	0.0943	0.1609	0.1041	0.56	0.11	2.81	0.00	0.03	0.07		
4	0.0732	5.2820	0.0003	0.0118	0.3223	0.3105	0.01	0.02	53.60	0.00	0.00	0.12	Fe oxides	
5	0.2548	5.0951	0.0004	0.0086	0.3115	0.3296	0.05	0.05	74.89	0.00	0.00	0.13		
6	0.1146	5.2901	0.0010	0.1189	0.2796	0.1958	0.02	0.01	4.00	0.00	0.02	0.09		
7	0.4222	5.0038	0.0013	0.1083	0.2692	0.1952	0.08	0.01	4.29	0.00	0.02	0.09		
8	0.8836	4.5689	0.0017	0.0861	0.2667	0.1930	0.19	0.02	5.34	0.00	0.02	0.10		
9	0.7396	4.9005	0.0376	0.1550	0.1067	0.0607	0.15	0.24	1.08	0.01	0.03	0.03		
10	0.0547	5.4463	0.0006	0.4984	0.0000	0.0000	0.01	0.00	0.00	0.00	0.09	0.00	Al oxides	
11	0.0154	5.6467	0.0004	0.3375	0.0000	0.0000	0.00	0.00	0.00	0.00	0.06	0.00		
12	0.2683	5.1444	0.0068	0.5804	0.0000	0.0000	0.05	0.01	0.00	0.00	0.11	0.00		
13	0.5141	4.9230	0.0023	0.5606	0.0000	0.0000	0.10	0.00	0.00	0.00	0.11	0.00		
14	0.1335	5.5285	0.1186	0.2192	0.0001	0.0000	0.02	0.54	0.00	0.02	0.04	0.00	Phyllosilicates	
15	0.3990	5.2662	0.0840	0.2505	0.0002	0.0001	0.08	0.34	0.00	0.02	0.05	0.00		
16	0.8902	4.7512	0.0541	0.3043	0.0002	0.0001	0.19	0.18	0.00	0.01	0.06	0.00		
17	0.0539	5.7216	0.1176	0.1063	0.0005	0.0001	0.01	1.11	0.01	0.02	0.02	0.00		
18	0.1745	5.5891	0.1065	0.1294	0.0005	0.0002	0.03	0.82	0.00	0.02	0.02	0.00		

Table S2: Characteristics of the 20 mass signature classes identified in the resin-embedded sample containing Quartz, Illite, Goethite, and spruce needle (Figure S3). Mean normalized counts (MNC) give the average MNC values of all pixels that were assigned to a given mass signature class (compare figure S4). Ratios were calculated with the average MNC values.

Mass signature class	Mean normalized counts [MNC]						Ratios							Compound groups	Colour
	^{12}C	^{16}O	$^{12}C^{14}N$	^{28}Si	$^{27}Al^{16}O$	$^{56}Fe^{16}O$	C/O	N/O	Si/Al	Si/O	Fe/Si	Fe/Al	C/N		
1	4.0593	1.4989	0.4166	0.0155	0.0096	0.0001	2.71	0.28	1.61	0.01	0.00	0.01	9.74	Resin	
2	3.6083	2.2047	0.1793	0.0048	0.0028	0.0001	1.64	0.08	1.73	0.00	0.03	0.05	20.13		
3	3.2234	2.1812	0.5861	0.0042	0.0048	0.0002	1.48	0.27	0.86	0.00	0.05	0.05	5.50		
4	3.0636	2.4999	0.4263	0.0041	0.0058	0.0002	1.23	0.17	0.71	0.00	0.06	0.04	7.19		
5	2.6379	2.9329	0.4152	0.0051	0.0086	0.0004	0.90	0.14	0.59	0.00	0.07	0.04	6.35		
6	2.6183	1.8952	1.4728	0.0052	0.0083	0.0002	1.38	0.78	0.63	0.00	0.04	0.02	1.78		
7	1.0742	1.0460	3.8679	0.0026	0.0093	0.0000	1.03	3.70	0.28	0.00	0.02	0.00	0.28	POM	
8	0.7896	1.6606	3.5385	0.0062	0.0051	0.0001	0.48	2.13	1.23	0.00	0.01	0.02	0.22		
9	1.6486	1.4980	2.8444	0.0037	0.0052	0.0001	1.10	1.90	0.70	0.00	0.02	0.02	0.58		
10	1.4398	2.6603	1.8684	0.0153	0.0156	0.0007	0.54	0.70	0.98	0.01	0.04	0.04	0.77		
11	0.7799	4.0260	1.1062	0.0392	0.0475	0.0011	0.19	0.27	0.83	0.01	0.03	0.02	0.71	Phyllosilicates	
12	0.2940	5.4242	0.1435	0.0780	0.0587	0.0016	0.05	0.03	1.33	0.01	0.02	0.03	2.05		
13	0.0831	5.7638	0.0345	0.0644	0.0539	0.0004	0.01	0.01	1.19	0.01	0.01	0.01	2.41		
14	0.7425	4.9380	0.1693	0.0625	0.0817	0.0060	0.15	0.03	0.76	0.01	0.10	0.07	4.38		
15	0.6659	4.6708	0.4988	0.0574	0.1051	0.0020	0.14	0.11	0.55	0.01	0.03	0.02	1.33		
16	1.2151	4.3442	0.3067	0.0586	0.0724	0.0031	0.28	0.07	0.81	0.01	0.05	0.04	3.96		
17	1.7421	3.2699	0.9434	0.0195	0.0242	0.0009	0.53	0.29	0.81	0.01	0.05	0.04	1.85		
18	2.0107	3.5629	0.3734	0.0187	0.0327	0.0016	0.56	0.10	0.57	0.01	0.08	0.05	5.38		
19	0.0215	5.8373	0.0107	0.1298	0.0006	0.0000	0.00	0.00	213.90	0.02	0.00	0.04	2.02	Quarz	
20	0.1926	5.6383	0.0346	0.1283	0.0060	0.0001	0.03	0.01	21.53	0.02	0.00	0.02	5.57		

Table S3: Characteristics of the 30 mass signature classes. Mean normalized counts (MNC) give the average MNC values of all pixels that were assigned to a given mass signature class (compare figure S7). Ratios were calculated with these average MNC values. Total coverage gives the relative area that is covered by the given mass signature class across all 40 images (compare figure S8). For the grouping of the 30 mass signature classes in 10 compound groups please check figure S9. Colour defines the appearance of the class in figure 2 and figure S8.

Mass signature class	Mean normalized counts						Ratios							Total coverage	Compound groups	Colour
	^{12}C	^{16}O	$^{12}C^{14}N$	^{28}Si	$^{27}Al^{16}O$	$^{56}Fe^{16}O$	C/O	N/O	C/N	Si/Al	Si/O	Fe/Si	Fe/Al	[area %]		
1	4.9771	0.2632	0.7398	0.0104	0.0085	0.0011	18.91	2.81	6.73	1.22	0.04	0.10	0.12	0.02	Pores	
2	5.0859	0.4755	0.4109	0.0126	0.0142	0.0009	10.70	0.86	12.38	0.89	0.03	0.07	0.07	0.62		
3	5.0092	0.8376	0.1387	0.0072	0.0068	0.0005	5.98	0.17	36.11	1.06	0.01	0.08	0.08	2.39		
4	3.8107	1.3657	0.7565	0.0298	0.0359	0.0015	2.79	0.55	5.04	0.83	0.02	0.05	0.04	3.34		
5	1.0115	1.3709	3.5823	0.0066	0.0276	0.0010	0.74	2.61	0.28	0.24	0.00	0.16	0.04	3.83	POM	
6	0.2222	0.5601	5.2111	0.0019	0.0046	0.0002	0.40	9.30	0.04	0.41	0.00	0.09	0.04	3.65		
7	0.5533	2.6001	2.7682	0.0207	0.0562	0.0015	0.21	1.06	0.20	0.37	0.01	0.07	0.03	2.61	OM + Al-rich phyllosilicates	
8	0.5034	3.5187	1.8386	0.0314	0.1054	0.0025	0.14	0.52	0.27	0.30	0.01	0.08	0.02	3.85		
9	0.0925	5.3420	0.2806	0.0508	0.2277	0.0063	0.02	0.05	0.33	0.22	0.01	0.12	0.03	2.70	Al-rich phyllo-silicates + OM	
10	0.1370	4.7140	0.9489	0.0412	0.1555	0.0034	0.03	0.20	0.14	0.26	0.01	0.08	0.02	11.06		
11	0.2495	5.0129	0.5988	0.0442	0.0843	0.0103	0.05	0.12	0.42	0.53	0.01	0.23	0.12	1.18	Al-rich mineral grains	
12	0.0771	5.6335	0.1210	0.0671	0.0945	0.0068	0.01	0.02	0.64	0.71	0.01	0.10	0.07	6.56		
13	0.0453	5.3666	0.4762	0.0565	0.0531	0.0022	0.01	0.09	0.10	1.06	0.01	0.04	0.04	6.24		
14	0.0177	5.8088	0.0636	0.0968	0.0117	0.0014	0.00	0.01	0.28	8.30	0.02	0.01	0.12	3.63		
15	3.2278	2.3509	0.2628	0.0806	0.0748	0.0030	1.37	0.11	12.28	1.08	0.03	0.04	0.04	1.52	(OM +) Si-rich phyllosilicates	
16	2.5208	2.1014	1.2516	0.0456	0.0782	0.0025	1.20	0.60	2.01	0.58	0.02	0.05	0.03	1.13		
17	2.3710	3.0249	0.3082	0.1276	0.1626	0.0057	0.78	0.10	7.69	0.78	0.04	0.04	0.04	0.58		
18	1.9906	3.3400	0.4512	0.1050	0.1089	0.0043	0.60	0.14	4.41	0.96	0.03	0.04	0.04	1.90		
19	1.3033	4.1982	0.2003	0.1476	0.1442	0.0064	0.31	0.05	6.51	1.02	0.04	0.04	0.04	3.18	Si-rich phyllo-silicates + OM	
20	0.8572	4.2038	0.5606	0.1548	0.2163	0.0073	0.20	0.13	1.53	0.72	0.04	0.05	0.03	1.00		
21	0.5667	4.9660	0.1312	0.1533	0.1744	0.0083	0.11	0.03	4.32	0.88	0.03	0.05	0.05	5.53	Si-rich phyllosilicates	
22	0.2074	5.3696	0.0775	0.1404	0.1968	0.0083	0.04	0.01	2.67	0.71	0.03	0.06	0.04	1.93		
23	0.0814	5.6039	0.0133	0.2461	0.0535	0.0018	0.01	0.00	6.14	4.60	0.04	0.01	0.03	10.23	Si-rich mineral grains	
24	0.0305	5.7434	0.0081	0.2035	0.0135	0.0010	0.01	0.00	3.78	15.06	0.04	0.01	0.08	19.65		
25	0.0503	5.4009	0.0066	0.5341	0.0068	0.0013	0.01	0.00	7.61	78.25	0.10	0.00	0.19	1.46		
26	0.0441	4.4693	0.0052	1.4660	0.0074	0.0079	0.01	0.00	8.41	198.33	0.33	0.01	1.07	0.01		
27	0.2792	5.5370	0.0167	0.0721	0.0729	0.0222	0.05	0.00	16.74	0.99	0.01	0.31	0.30	0.08		
28	0.2451	5.3538	0.0424	0.1317	0.0720	0.1550	0.05	0.01	5.79	1.83	0.02	1.18	2.15	0.04	Metal oxides	
29	0.1298	5.5363	0.0286	0.0343	0.1400	0.1309	0.02	0.01	4.53	0.25	0.01	3.81	0.93	0.04		
30	0.0460	5.6450	0.0558	0.0306	0.0595	0.1630	0.01	0.01	0.82	0.51	0.01	5.32	2.74	0.07		

Table S4: Relative area that is covered by a specific mass signature class in each of the 40 images (compare Figure 1 and 2 and figure S8) - each line sums up to 100%. For the grouping of the 30 mass signature classes in 10 compound groups please check figure S7 and S9. For more details on the clustering of the 40 images into three microdomains please check figure S10.

NanoSIMS Image	Mass signature class coverage [area %]																												Microdomain
	Pores				POM		OM + Al-rich phyllosilicates		Al-rich phyllosilicates + OM		Al-rich mineral grains				(OM +) Si-rich phyllosilicates				Si-rich phyllosilicates + OM		Si-rich phyllosilicates		Si-rich mineral grains				Metal oxides			
	1	2	3	4	5	6	7	8	9	10	11	12	13	14	15	16	17	18	19	20	21	22	23	24	25	26	27	28	29	30	
A5	0.00	0.00	0.00	11.37	22.41	1.37	3.37	8.61	11.07	23.62	2.30	4.06	3.28	0.48	0.00	3.11	0.06	1.32	0.39	1.87	0.42	0.50	0.08	0.31	0.00	0.00	0.00	0.00	0.00	0.00	C
B4	0.00	0.00	7.37	2.34	0.00	0.00	0.00	0.00	0.00	0.00	0.00	0.09	0.00	0.00	1.96	0.01	0.48	1.38	3.14	0.02	4.75	1.44	39.04	37.97	0.00	0.00	0.01	0.00	0.00	0.00	A
B6	0.00	0.00	3.78	6.96	1.55	0.05	1.01	1.77	0.88	2.49	1.43	13.72	0.74	0.03	2.57	0.90	1.11	3.90	9.08	1.55	18.90	6.32	11.39	9.55	0.10	0.00	0.16	0.02	0.06	0.00	A
C5	0.00	0.00	0.00	0.00	0.00	0.00	0.00	0.00	0.00	0.00	0.00	0.00	0.00	0.00	0.00	0.00	0.00	0.02	0.05	0.00	0.05	0.00	9.02	90.86	0.00	0.00	0.00	0.00	0.00	0.00	pure mineral
C7	0.00	0.00	0.00	0.03	0.40	0.00	0.45	1.17	1.98	6.00	0.76	7.07	4.42	40.78	0.00	0.14	0.00	0.20	0.12	0.20	0.06	0.01	0.00	35.66	0.00	0.00	0.01	0.00	0.00	0.53	B
D4	0.00	0.01	2.23	6.51	0.00	0.00	0.00	0.18	0.15	0.21	0.09	7.90	0.00	0.10	4.09	0.73	1.81	3.66	9.15	1.30	16.04	4.09	21.31	14.18	3.13	0.00	1.50	0.36	0.73	0.53	A
D6	0.00	0.13	3.46	3.73	0.00	0.00	0.00	0.00	0.00	0.00	0.00	2.03	0.00	0.25	4.13	0.17	1.29	2.77	6.56	0.11	12.65	6.67	5.73	49.69	0.48	0.00	0.07	0.08	0.01	0.00	A
E3	0.00	0.00	0.00	0.00	0.18	0.05	0.27	3.53	0.00	84.56	6.89	0.00	4.53	0.00	0.00	0.00	0.00	0.00	0.00	0.00	0.00	0.00	0.00	0.00	0.00	0.00	0.00	0.00	0.00	0.00	pure mineral
E5	0.00	0.01	0.00	1.57	13.12	39.37	5.44	7.40	2.39	17.30	1.39	4.19	5.97	0.57	0.00	0.86	0.00	0.13	0.03	0.27	0.00	0.00	0.00	0.00	0.00	0.00	0.00	0.00	0.00	0.00	C
F1	0.00	0.00	0.00	0.00	10.94	0.44	35.49	33.67	0.00	15.62	0.45	0.11	3.04	0.07	0.00	0.00	0.00	0.00	0.00	0.00	0.00	0.00	0.00	0.17	0.00	0.00	0.00	0.00	0.00	0.00	C
F2	0.00	0.00	0.00	0.00	20.51	76.33	1.79	0.54	0.00	0.33	0.00	0.08	0.26	0.15	0.00	0.00	0.00	0.00	0.00	0.00	0.00	0.00	0.00	0.00	0.00	0.00	0.00	0.00	0.00	0.00	C
F4	0.00	0.20	15.68	5.39	0.00	0.00	0.07	0.17	0.83	0.61	0.11	4.58	0.14	0.09	4.16	0.47	0.98	4.04	7.21	0.70	11.54	5.98	8.45	27.56	0.73	0.00	0.20	0.04	0.05	0.00	A
F6	0.00	0.76	4.43	8.08	0.00	0.00	0.00	0.05	0.23	0.19	0.13	4.05	0.02	0.00	5.80	0.96	1.73	5.60	9.54	1.07	15.43	5.81	19.57	16.17	0.33	0.00	0.01	0.03	0.00	0.00	A
G1	0.00	0.00	0.00	0.10	0.81	0.53	1.14	2.34	8.44	4.89	1.61	17.52	1.06	5.48	0.00	5.76	0.04	3.18	1.40	2.16	3.84	0.81	0.05	38.52	0.00	0.00	0.01	0.01	0.10	0.19	B
G2	0.00	0.00	0.00	0.00	0.51	0.09	0.44	0.43	0.00	1.24	0.79	1.99	94.51	0.00	0.00	0.00	0.00	0.00	0.00	0.00	0.00	0.00	0.00	0.00	0.00	0.00	0.00	0.00	0.00	0.00	pure mineral
G3	0.00	0.00	0.00	0.00	14.88	6.97	9.06	14.41	0.02	45.58	0.63	0.00	8.45	0.00	0.00	0.00	0.00	0.00	0.00	0.00	0.00	0.00	0.00	0.00	0.00	0.00	0.00	0.00	0.00	0.00	C
G5	0.00	0.04	0.08	18.15	1.53	0.93	1.05	2.11	9.91	4.41	1.09	7.86	0.75	1.14	2.85	8.14	0.64	5.52	3.42	2.85	8.49	5.73	0.65	12.67	0.00	0.00	0.01	0.00	0.00	0.00	A
G7	0.00	0.00	0.00	0.97	11.73	0.22	6.71	10.33	16.38	29.95	1.84	10.25	6.93	0.00	0.00	2.74	0.00	0.29	0.04	1.50	0.07	0.03	0.00	0.00	0.00	0.00	0.00	0.00	0.00	0.00	C
H1	0.00	0.00	0.00	0.00	1.06	0.00	2.19	6.17	22.40	13.68	2.64	26.06	3.41	10.91	0.00	3.04	0.00	0.95	0.26	2.05	1.20	0.28	0.09	3.07	0.00	0.00	0.01	0.00	0.02	0.50	C
H2	0.00	0.00	0.00	0.06	0.27	0.00	2.24	5.06	0.00	3.51	12.57	47.09	16.90	0.65	0.02	2.69	0.00	4.15	2.16	1.96	0.68	0.00	0.00	0.00	0.00	0.00	0.01	0.00	0.00	0.00	C
H4	0.00	0.78	4.12	6.97	0.00	0.00	0.00	0.08	0.38	0.19	0.05	0.91	0.07	0.01	3.56	0.85	1.29	2.89	5.89	0.90	12.94	4.58	41.74	10.74	1.04	0.00	0.00	0.00	0.00	0.00	A
H6	0.00	0.00	0.00	0.00	0.00	0.00	0.00	0.00	0.00	0.00	0.00	0.00	0.00	0.00	0.00	0.00	0.00	0.00	0.00	0.00	0.01	0.00	14.06	85.92	0.00	0.00	0.00	0.00	0.00	0.00	pure mineral
I2	0.00	0.00	0.00	0.00	12.19	17.71	8.85	13.14	0.07	38.19	1.53	0.79	7.52	0.00	0.00	0.00	0.00	0.00	0.00	0.00	0.00	0.00	0.00	0.00	0.00	0.00	0.00	0.00	0.00	0.00	C
I3	0.00	0.00	0.00	0.00	13.11	0.39	7.04	9.29	1.57	32.64	1.10	5.93	28.46	0.46	0.00	0.00	0.00	0.00	0.00	0.00	0.00	0.00	0.00	0.00	0.00	0.00	0.00	0.00	0.00	0.00	C
I5	0.77	6.93	2.99	3.59	0.04	0.00	0.02	0.18	0.00	0.03	0.00	0.04	0.00	0.00	1.21	2.33	1.95	1.66	4.24	5.46	7.48	1.66	14.20	0.03	44.23	0.52	0.00	0.43	0.00	0.00	A
I7	0.00	0.00	0.00	0.14	4.76	0.25	2.90	5.35	8.85	18.91	1.96	11.20	10.77	34.07	0.00	0.16	0.00	0.03	0.01	0.30	0.01	0.00	0.00	0.35	0.00	0.00	0.00	0.00	0.00	0.00	C
J2	0.00	0.00	0.00	0.00	8.23	0.91	5.11	10.16	0.38	39.89	2.73	2.86	29.70	0.02	0.00	0.00	0.00	0.00	0.00	0.00	0.00	0.00	0.00	0.00	0.00	0.00	0.00	0.00	0.00	0.00	C
J4	0.00	0.13	2.60	4.32	0.30	0.00	0.21	0.44	0.14	0.29	0.18	1.68	0.06	0.03	2.59	0.99	1.15	3.33	6.02	1.38	10.26	3.78	39.83	16.99	3.29	0.00	0.00	0.00	0.02	0.00	A
J6	0.00	0.40	9.33	11.62	1.40	0.00	0.45	0.89	0.31	0.53	0.44	4.42	0.24	0.07	5.07	1.91	1.41	5.31	8.55	1.79	16.38	6.49	8.40	13.00	0.43	0.00	0.55	0.10	0.44	0.08	A
J8	0.00	0.00	0.00	0.01	0.85	0.00	1.10	2.26	0.79	1.84	1.22	23.45	5.04	28.78	0.00	0.13	0.00	0.15	0.08	0.63	0.10	0.09	0.00	33.48	0.00	0.00	0.00	0.00	0.00	0.00	B
K3	0.00	0.05	0.10	7.38	0.06	0.00	0.12	0.40	1.83	0.71	0.56	5.34	0.35	0.05	0.67	1.38	0.25	2.26	2.65	0.92	5.23	2.38	14.90	52.34	0.09	0.00	0.00	0.00	0.00	0.00	A
K5	0.00	14.69	10.60	7.51	2.66	0.18	1.57	2.11	0.19	2.15	0.07	0.08	0.23	0.00	3.29	2.98	3.88	2.95	8.71	5.91	15.33	4.63	9.74	0.05	0.47	0.00	0.00	0.01	0.02	0.00	A
K7	0.00	0.00	0.00	0.24	3.87	0.14	2.79	4.49	10.42	32.62	0.77	23.33	10.84	9.49	0.00	0.54	0.00	0.11	0.01	0.19	0.01	0.01	0.01	0.13	0.00	0.00	0.00	0.00	0.00	0.00	C
K9	0.00	0.00	0.00	1.12	5.61	0.37	2.61	6.28	7.74	21.11	1.81	11.48	4.53	12.79	0.00	0.91	0.01	0.45	0.12	1.10	0.09	0.08	0.07	21.16	0.00	0.00	0.00	0.00	0.00	0.58	B
L4	0.00	0.00	3.68	3.73	0.03	0.00	0.03	0.04	0.13	0.11	0.07	3.66	0.07	0.04	3.85	0.48	1.05	4.58	9.64	0.63	14.49	3.55	25.82	22.79	1.27	0.00	0.18	0.09	0.00	0.00	A
M5	0.00	0.09	4.82	5.02	0.00	0.00	0.00	0.00	0.02	0.08	0.05	1.59	0.01	0.32	4.56	0.13	0.81	4.33	8.57	0.33	11.54	1.05	29.33	26.36	0.76	0.00	0.22	0.02	0.00	0.00	A
N4	0.00	0.00	0.83	2.47	0.00	0.00	0.00	0.01	0.08	0.05	0.02	2.33	0.01	0.04	2.23	0.51	0.85	2.54	4.92	0.41	8.58	2.71	4.90	66.40	0.00	0.00	0.03	0.02	0.05	0.00	A
N6	0.00	0.02	16.64	8.77	0.29	0.00	0.23	0.50	0.14	0.55	0.12	2.50	0.16	0.02	4.18	0.76	1.09	3.44	6.15	0.74	9.40	3.07	23.80	17.12	0.20	0.00	0.01	0.04	0.00	0.06	A
O5	0.00	0.00	0.00	0.02	0.00	0.00	0.00	0.00	0.00	0.00	0.00	0.00	0.00	0.14	0.17	0.01	0.00	0.35	0.59	0.00	0.38	0.00	47.13	50.88	0.32	0.00	0.00	0.00	0.00	0.00	A
P4	0.00	0.12	1.71	4.01	0.13	0.00	0.15	0.29	0.26	0.55	0.04	3.26	0.04	0.29	2.95	1.06	1.13	3.59	6.80	1.43	12.01	4.32	17.85	36.81	0.47	0.00	0.02	0.34	0.16	0.21	A

Figure S1: Test data set 1 for the identification and discrimination of seven pure standard materials (Table S1). All seven standard materials were attached to an individual adhesive carbon film and measured separately. The results are shown as false color images (upper set; red: ^{28}Si, green: $^{27}Al^{16}O$, blue: $^{56}Fe^{16}O$) and classification images (lower set). Images a, b, and c show synthesized iron oxide minerals (Goethite) with increasing aluminum substitution (from left to right). Image d to g show minerals from natural mineral deposits – d: industrial iron oxide (Goethite), e: aluminum oxide (Boehmite), f: phyllosilicates (Illite), and g: phyllosilicates (Montmorillonite). All materials were attached to adhesive carbon film.

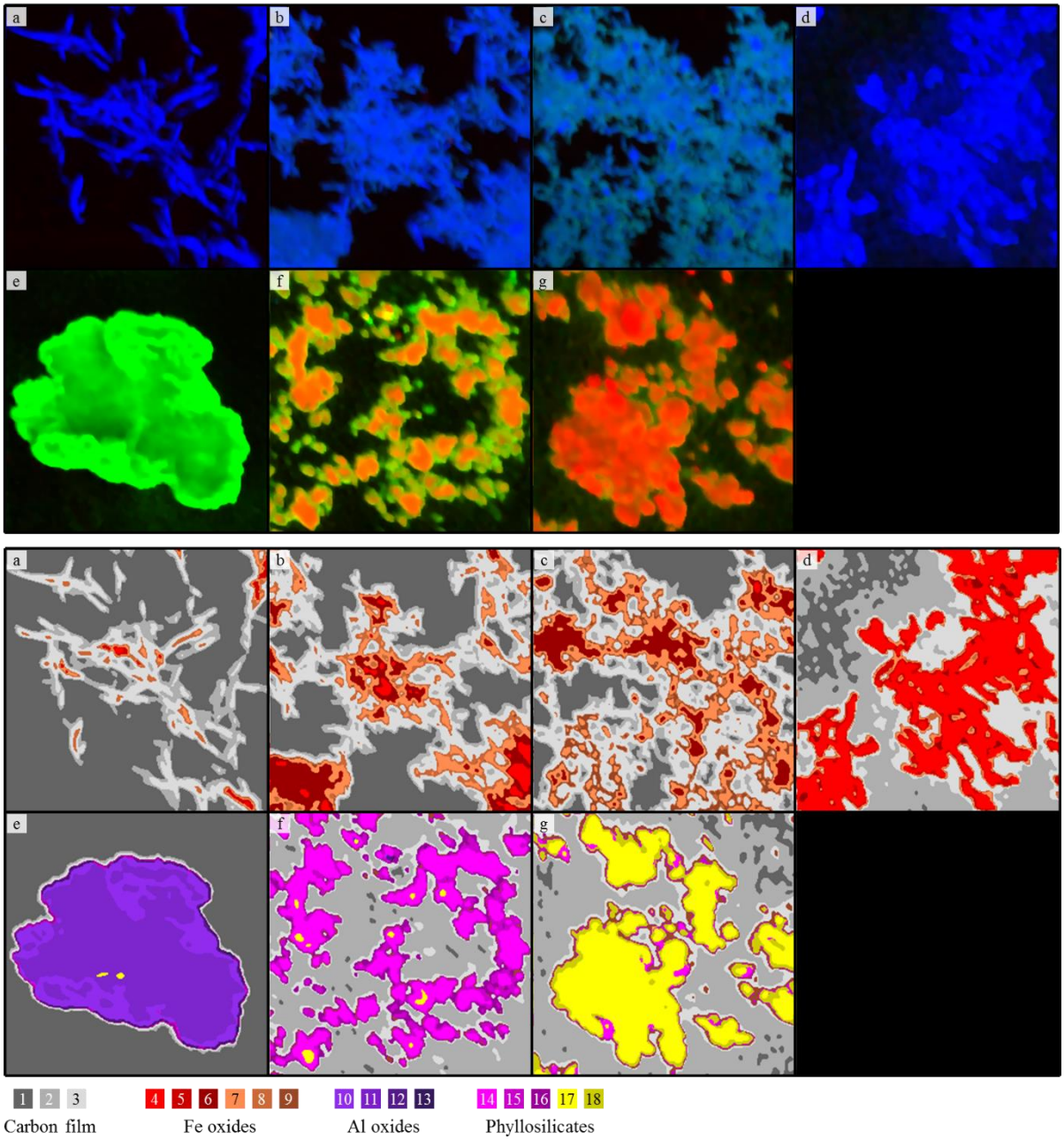

Figure S2: Elemental composition of the 18 mass signature classes extracted from NanoSIMS images of test data set 1 (Figure S1 and table S1) shown as mean normalized counts (MNC) for all six secondary ions (^{12}C, ^{16}O, ^{28}Si, $^{27}Al^{16}O$, $^{56}Fe^{16}O$, $^{56}Fe^{16}O_2$). The 18 mass signature classes are grouped in five compound groups.

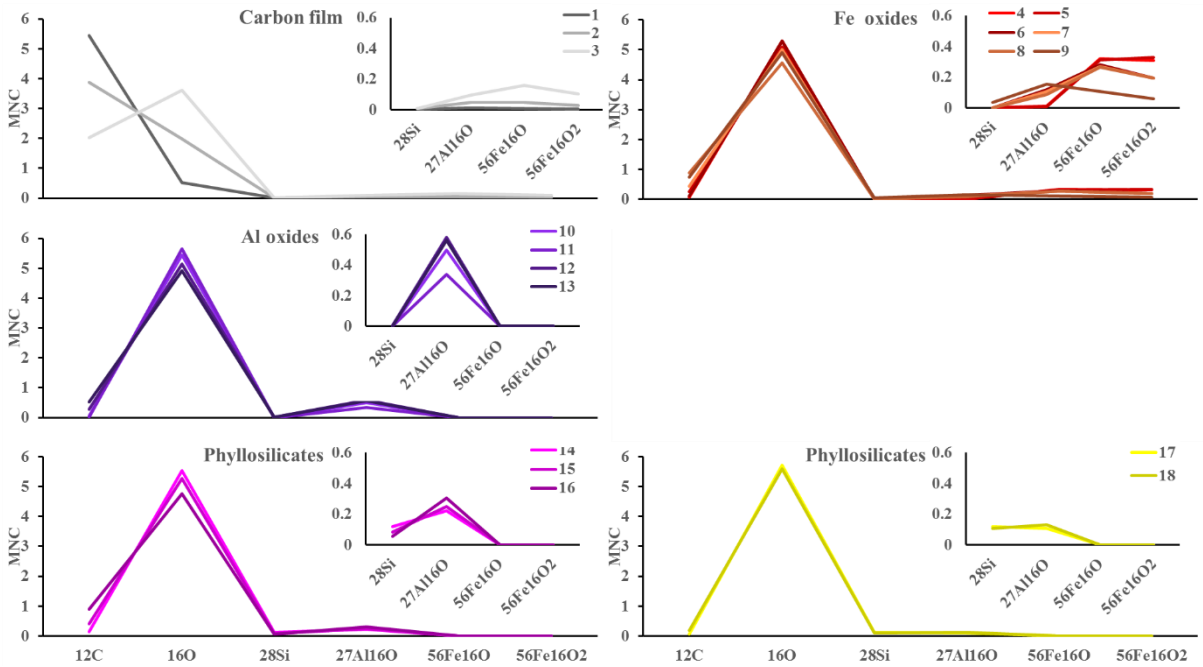

Figure S3: Test data set 2 for the identification and discrimination of three standard materials (Spruce needle, phyllosilicates (Illite), and Si oxide (Quartz)), which were mixed together, resin-embedded, the resulting block cut, and polished. The results are shown as false color images (upper set; red: ^{28}Si, green: $^{12}C^{14}N$, blue: $^{27}Al^{16}O$) and classification images (lower set) of 18 NanoSIMS measurements taken at different locations on the cut, and polished resin block (please see table S2 and figure S4).

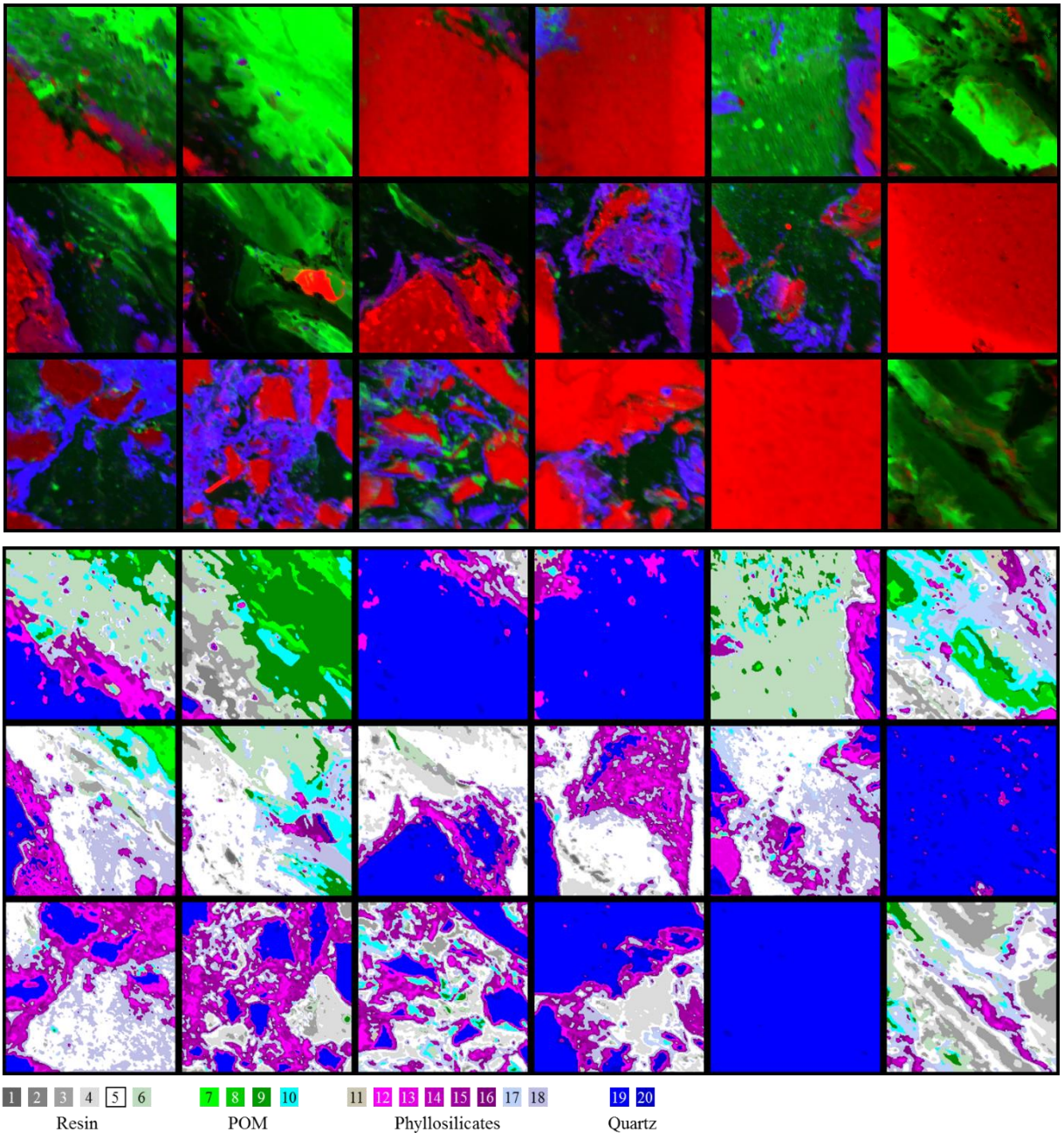

Figure S4: Elemental composition of the 20 mass signature classes extracted from 18 NanoSIMS measurements taken at different locations on test data set 2 (Spruce needle, phyllosilicates (Illite), and Si oxide (Quartz); Figure S3 and table S2) shown as mean normalized counts (MNC) for all six secondary ions (^{12}C, ^{16}O, $^{12}C^{14}N$, ^{28}Si, $^{27}Al^{16}O$, $^{56}Fe^{16}O$). The 20 mass signature classes are grouped in four compound groups.

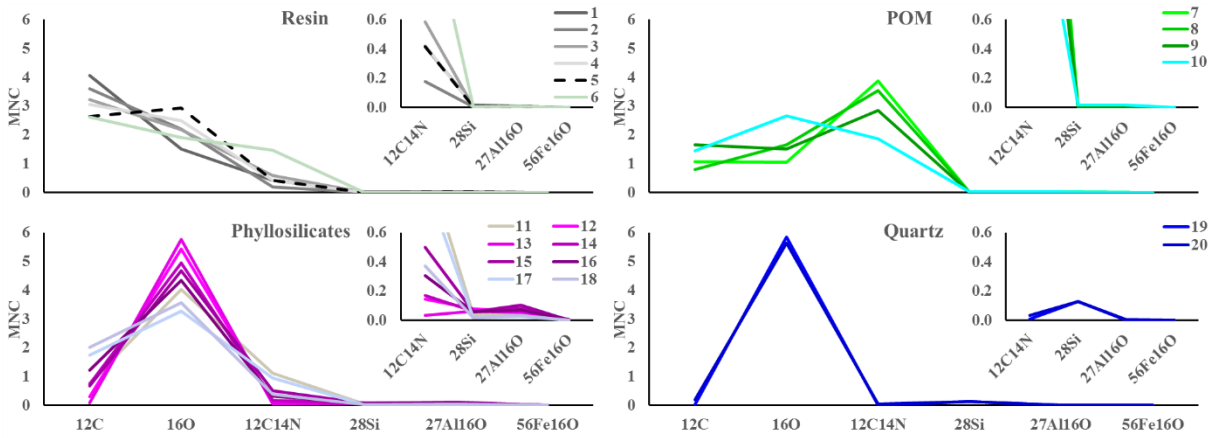

Figure S5: Effect of preprocessing and normalization on 40 NanoSIMS images as presented in false color composites (red = ^{28}Si, green = $^{12}C^{14}N$, blue = $^{27}Al^{16}O$) and on mass signatures of six selected classes. The left mosaic is built of 40 images of raw, non-normalized counts, and the right mosaic contains 40 images with preprocessed and normalized counts. In both mosaics, the 40 images are sorted into the three functional microdomains (Figure S10) and pure mineral images (Table S4). The four graphs below the mosaics show the mean and standard deviation for three classes from Microdomain A and three classes from Microdomains B+C as affected by pre-processing and normalization.

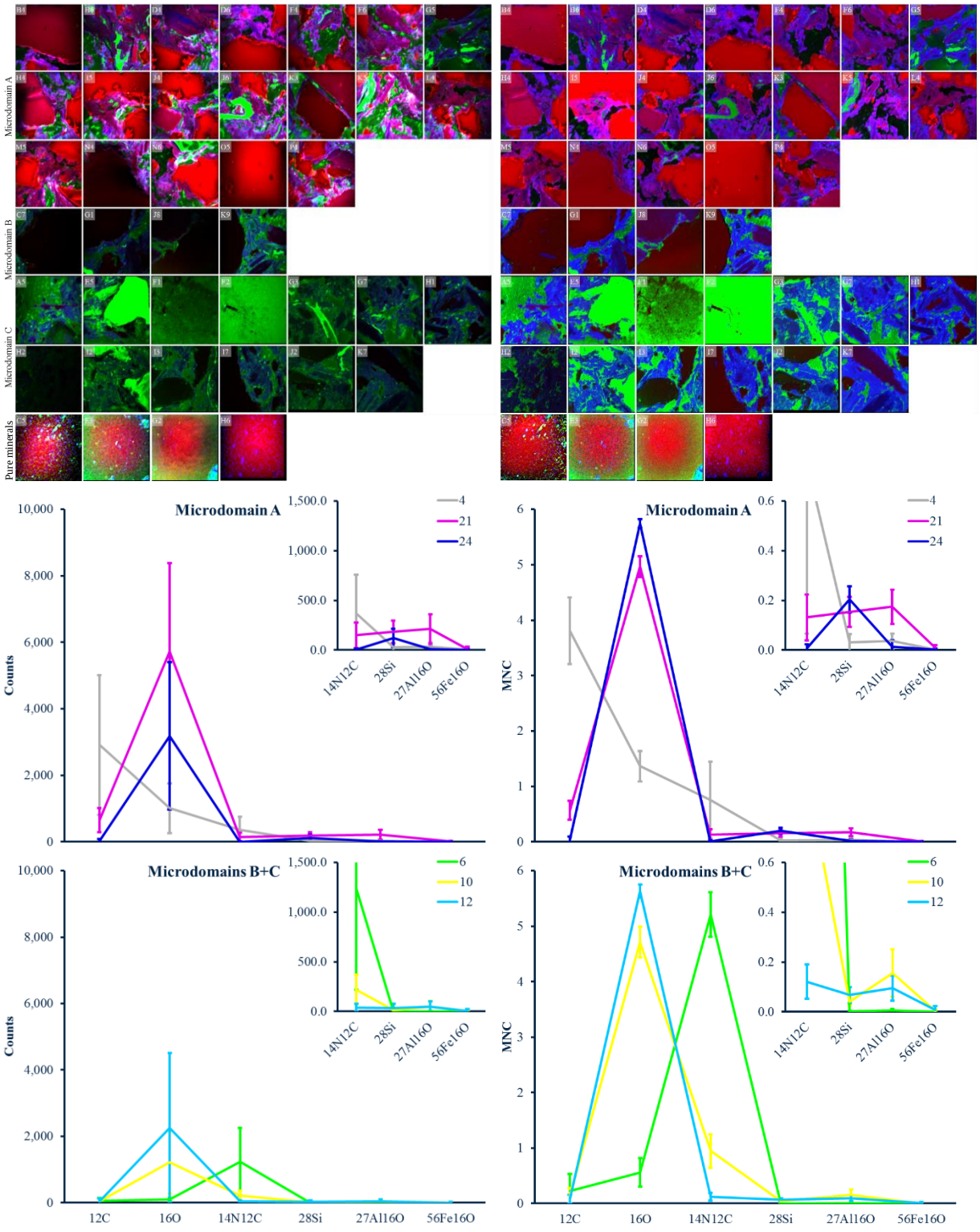

Figure S6: Elemental composition of the 30 mass signature classes shown as counts (no preprocessing and normalization was applied) for all six secondary ions (^{12}C, ^{16}O, $^{14}N^{12}C$, ^{28}Si, $^{27}Al^{16}O$, $^{56}Fe^{16}O$). The 30 mass signature classes are grouped in 10 compound groups, based on the cluster analysis shown in figure S9.

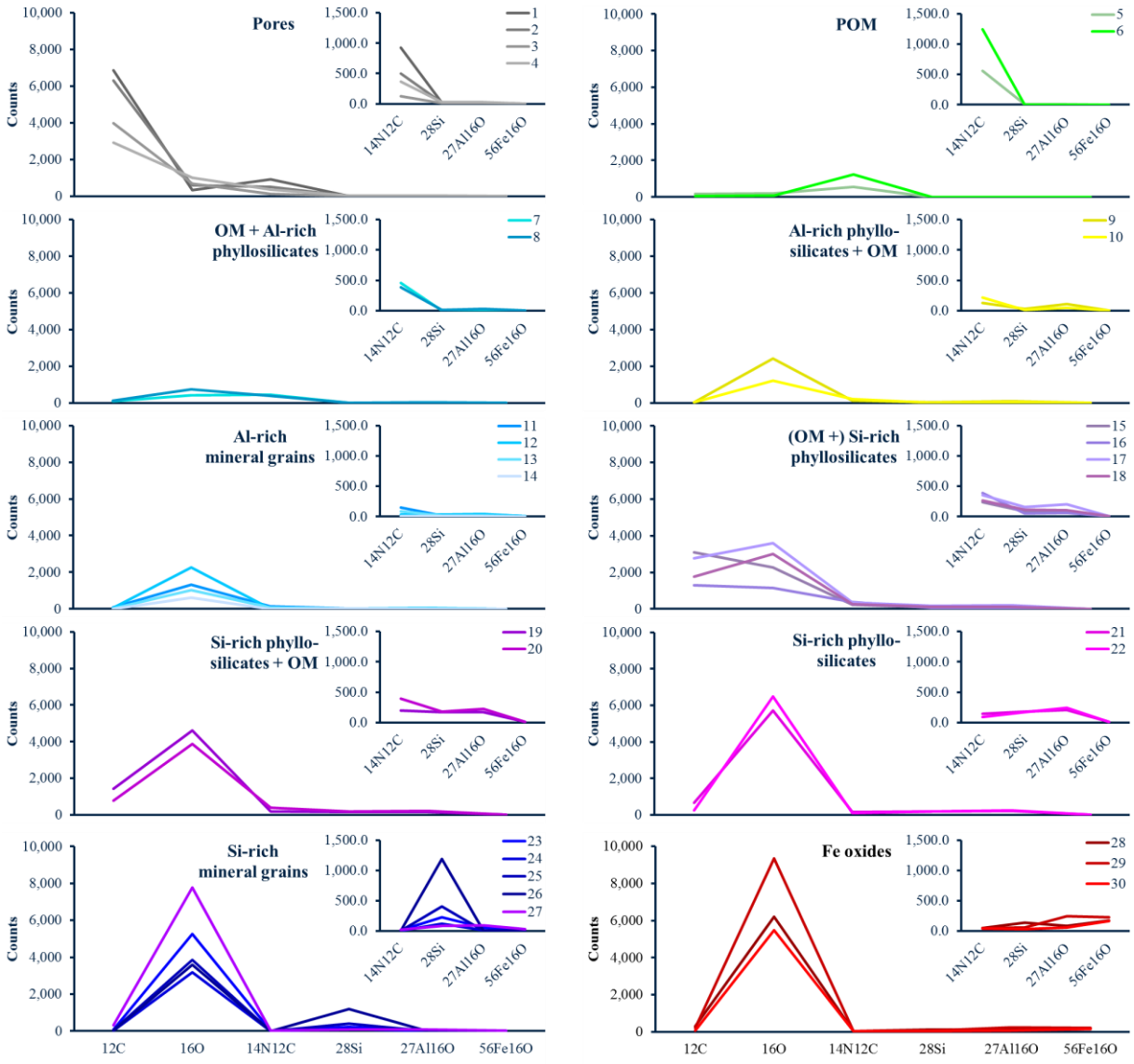

Figure S7: Elemental composition of the 30 mass signature classes shown as mean normalized counts (MNC) for all six secondary ions (^{12}C, ^{16}O, $^{14}N^{12}C$, ^{28}Si, $^{27}Al^{16}O$, $^{56}Fe^{16}O$). The 30 mass signature classes are grouped in 10 compound groups, based on the cluster analysis shown in figure S9.

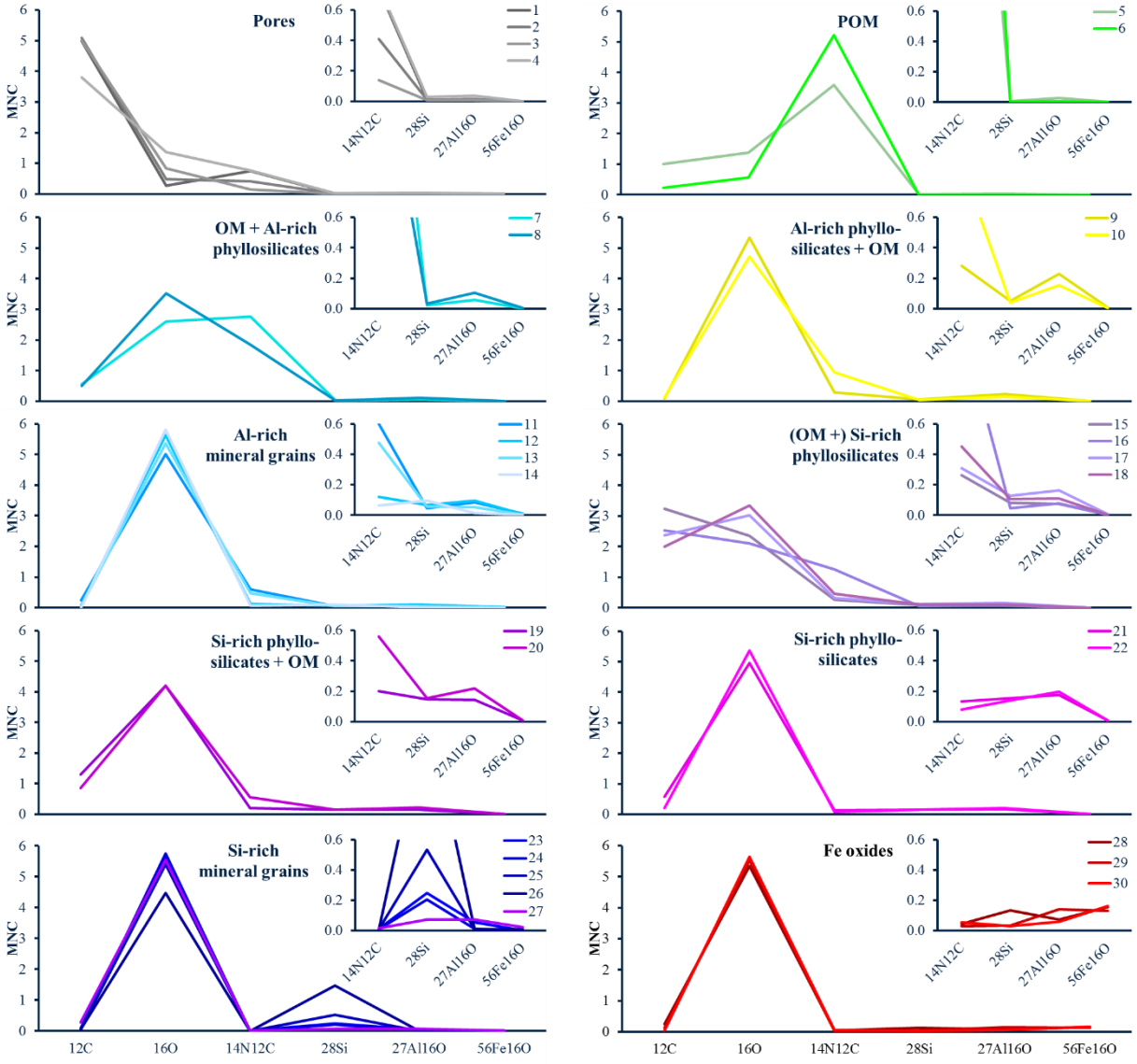

Figure S8: Classification images of 40 NanoSIMS measurements sorted into three functional microdomains and pure minerals (Table S4, figure S10). The 30 mass signature classes (Figure S7) are clustered in 10 compound groups (Figure S9).

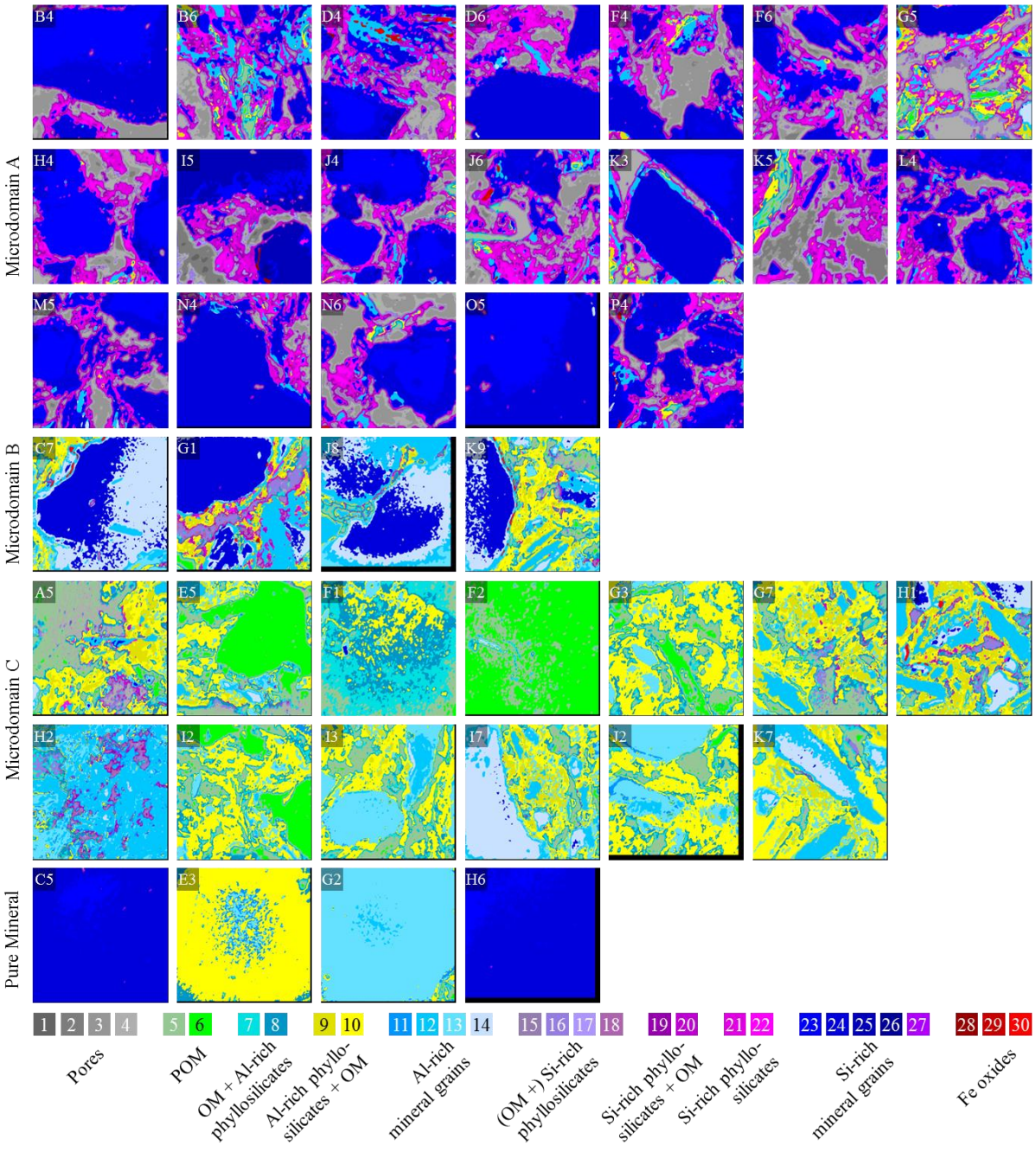

Figure S9: Clustering of the 30 mass signature classes into 10 compound groups. We used the mean normalized counts of all six secondary ions to group classes of similar mass signatures using a squared Euclidean distance approach (left diagram). 15 classes were similar in this first clustering step and were clustered in a second step based on the three secondary ions ^{28}Si, $^{27}Al^{16}O$, and $^{56}Fe^{16}O$ (right diagram).

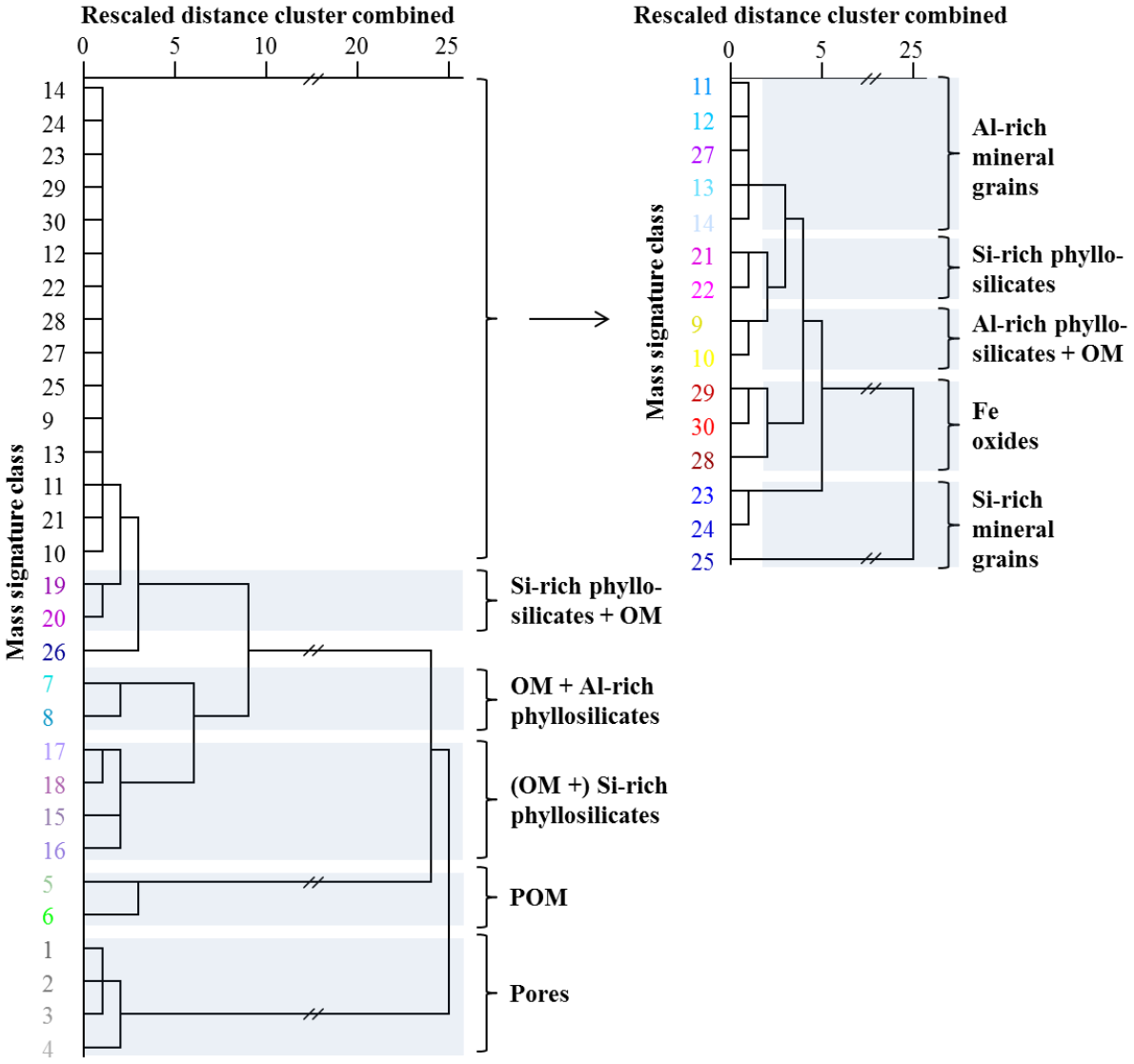

Figure S10: Clustering of 36 NanoSIMS images into three functional microdomains. The four measurements that covered only single mineral grains (C5, E3, G2, and H6) were not included. We used the relative coverages of the 30 mass signature classes in each image (Table S4) to group images with similar coverages using a squared Euclidean distance approach.

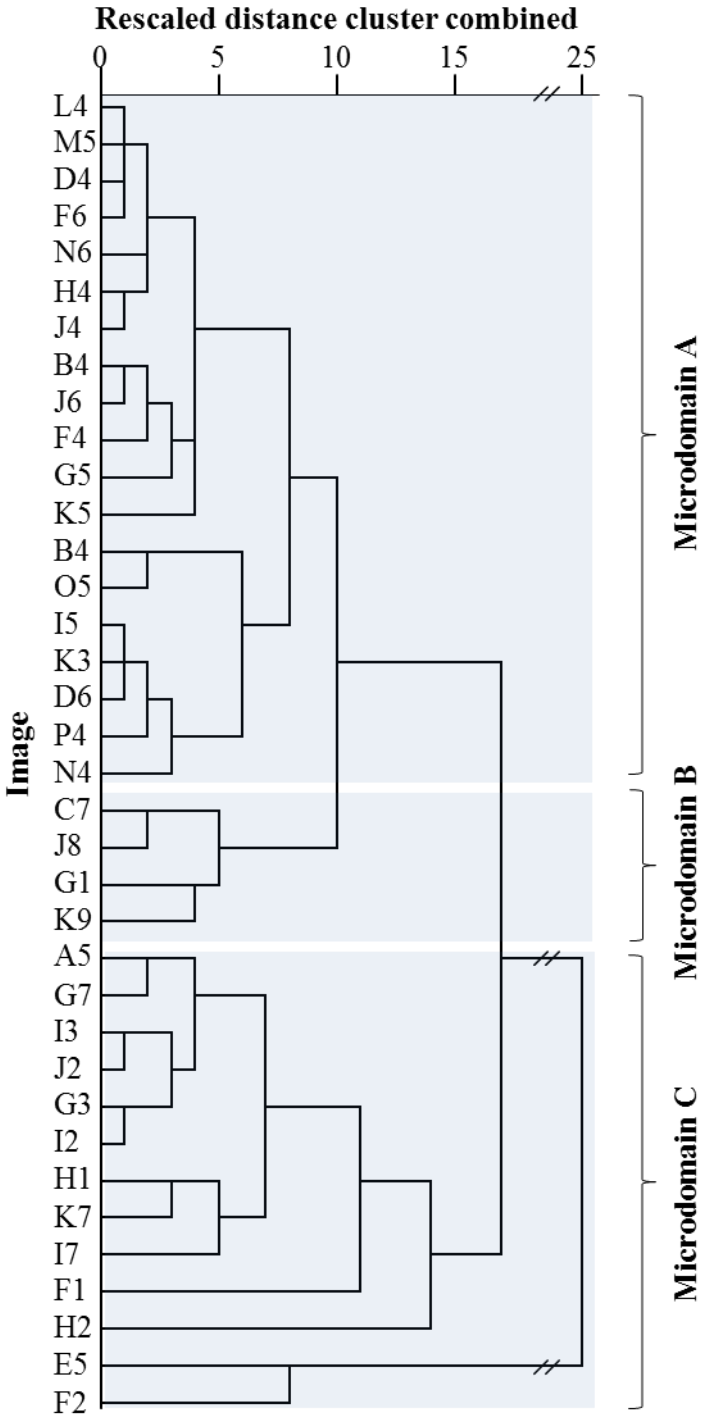

Figure S11: Energy-dispersive X-ray spectra of eight spots representative for the Si-rich minerals grains (upper left) and Si-rich phyllosilicates (lower left) and Al-rich mineral grains (upper right) and Al-rich phyllosilicates (lower right). We normalised each spectrum on its highest peak to allow a qualitative comparison between the different measurements. The code in the brackets following the class number give the NanoSIMS image were the spectrum was taken (Figure 1). The letters next to the peaks give the corresponding element.